3D Dark Blood MR Angiography of the Thoracic Vessels

Y-C. Chung[1], S. Cook[2], J. Park[3], M. Winner[2], R. Jerecic[4], and O. Simonetti[5]

[1]Siemens Medical Solutions USA, Inc., Columbus, Ohio, United States, [2]Ross Heart Hospital, [3]Siemens Medical Solutions, Germany, [4]Siemens Medical Solutions USA, Inc., [5]The Ohio State University

Introduction Evaluation of congenital heart disease and aortopathy is commonly performed by MRI due to its non-ionizing radiation and good soft tissue contrast. 3D angiography such as contrast enhanced MRA (ceMRA), bright blood and dark blood 3D TrueFISP [1-3] can depict the morphology of the great vessels. However after surgical repair involving placement of stents, closure devices and other metallic implants, gradient echo techniques have limited utility due to their sensitivity to susceptibility artifacts. Spin echo based methods such as 2D turbo spin echo and HASTE are the only alternatives in these cases. These 2D methods, on the other hand, provide limited anatomical coverage and suffer from long scan time [4] and partial volume effects. Slice positioning can be challenging in congenital cases due to the often complicated anatomy. We propose here a new, fast dark blood 3D turbo spin echo technique (aka SPACE) for imaging cardiothoracic anatomy and evaluate its potential for post-surgical follow-up in patients with stainless steel stents.

Method Sequence: The SPACE sequence has: 1) variable flip angle nonselective refocusing pulse train [5] that optimizes T1 contrast, disrupts even-echo rephasing and improves sampling efficiency; 2) strong crushers applied along the readout gradients suppressing flowing blood but not stationary tissues [6]; 3) systolic acquisition maximizing flow induced spin dephasing. No dark blood pulse is used. The sequence with navigator gating was implemented on a 1.5T clinical scanner (Magnetom Avanto, Siemens, Germany).
Imaging parameters: SPACE: TR/TE =1 RR interval/20ms; ETL=~30; parallel acquisition technique rate 2 (PAT2); NEX=2; 40-72 slices; bandwidth=600Hz/pixel; systolic acquisition; voxel size=$(1.2mm)^3$ (=1.7 mm^3) uninterpolated. 3D TrueFISP: 34 segments/RR interval; TR/TE= 3.3ms/1.4ms (asym echo); flip angle=90^o; PAT2; NEX=1; ~80 slices; bandwidth=700Hz/pixel; diastolic acquisition; voxel size=$(1.5mm)^2$ x 2mm (=4.2 mm^3) interpolated to $(0.75mm)^2$ x 1.3mm. Both sequences were ECG triggered and navigator gated.
Imaging: The study was approved by the institutional review board. In five healthy volunteer studies, aortic flow was measured to find the time when peak velocity commonly occurred. The trigger delay in SPACE acquisition was adjusted based on this timing for optimal blood suppression. Four patients who previously underwent surgery and known to have MR compatible metallic vascular stents were scanned using TrueFISP and SPACE. Imaging slabs were prescribed to cover the region of interest.
Evaluation: The volunteer data sets were visually assessed for image quality and blood suppression. In patients, the bright blood and dark blood angiograms were collected at different cardiac phases which precluded direct comparison of vessel lumen diameters. Instead, the two 3D angiograms from each patient were first registered in three dimensions using the "Fusion" software (Siemens Medical Solutions, Erlangen, Germany) and displayed side by side for image interpretation. Stent position was identified based on the signal void in TrueFISP images and the surgical record of each patient.

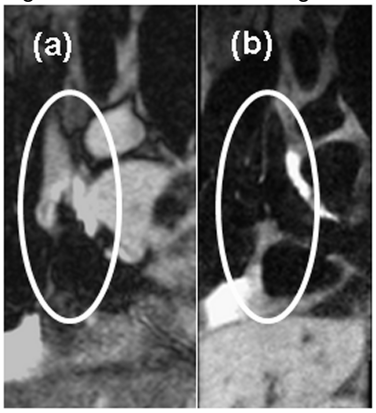

Fig 1: The patient has d-TGA and post-Mustard repair. Due to obstruction, two stainless steel stents were placed within the SVC baffle which goes to the left atrium. In (a), artifact in the TrueFISP image makes visualization of the regions near the metallic stent impossible. The dark blood image in (b) demonstrates stent patency.

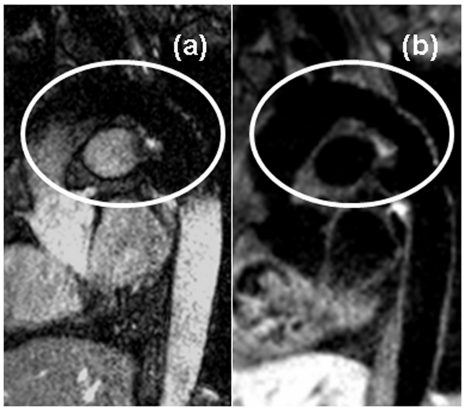

Fig 2: The patient with coarctation of the aorta had percutaneous intervention and stent placement due to stenosis at a site of previous surgical repair. In the TrueFISP image (a) the large signal void prevents assessment of stent patency. The dark blood image in (b) clearly suggests that the stent is patent.

Results Acquisitions were successful in all volunteers and patients. Imaging parameters for SPACE optimized from volunteer studies gave consistent image quality in patient studies. Broad coverage of the thick slab made positioning trivial in all cases. In patients, blood was suppressed with a trigger delay of ~40ms. No vessel pulsatility related artifact was observed, probably due to the nonselective refocusing pulses used in SPACE. In patients, the signal voids in TrueFISP images corresponded to the expected positions of the stents. The obvious large regions of signal void surrounding stent locations in TrueFISP images were dramatically smaller and apparently localized to the stent itself in the SPACE images. Stent-induced artifact was significantly more pronounced in TrueFISP than in SPACE. The average scan time, taking into account navigator efficiency, was ~10.8-15.8 s/partition, which was comparable to breathhold 2D TSE scan time per slice. Two clinical cases are shown in Fig.1-2.

Discussion Our initial experience with SPACE shows the clinical potential of the new technique. It improves the visualization of vessel patency and complements bright blood techniques for visualization of complex cardiothoracic anatomy. The high isotropic resolution helps depict vessel lumens in the presence of metallic stents not previously possible with gradient echo techniques. Studies have yet to be done to understand the extent of the artifacts from metallic stents in SPACE images.

Conclusion High resolution dark blood 3D MRA is possible with navigator SPACE. The technique is less sensitive to metallic artifacts compared to gradient echo techniques, making it a good technique to follow up patients with acquired or congenital aortic diseases.

References [1] Sorensen TS et al., Circulation 110:163-169, 2004. [2] Deshpande VS et al., Proc. 14th ISMRM, p.1935, 2006. [3] Koktzoglou IJ et al., AJR 189:966-972, 2007. [4] Gebker R et al., Int J Cardiovasc Imaging, 23(6): 747-756, 2007. [5] Mugler JP & Brookeman JR, Proc. 12th ISMRM, p.695, 2004. [6] Miyazaki M et al., Radiology 227:890-896, 2003.